



A comparative study of electronic and thermoelectric properties of bulk, 2D sheet and 1D wire of Silicon: an *ab-initio* study

H. Joshi¹, D. P. Rai², Sandeep¹, A. Shankar³, P. K. Patra⁴, R. K. Thapa¹

¹Department of Physics Mizoram University, Aizawl, India 796004

²Department of Physics, Pachhunga University College, Aizawl, India 796001

³Department of Physics, North Bengal University, Siliguri, Darjeeling, India.

⁴Faculty in Centre for Science Education, NEHU Shillong, 794022, India

Received 13 Oct 2016; Revised 21 Mar 2017; Accepted 18 May 2017

Abstract

We have made a comparative study of the electronic and thermoelectric properties of bulk, 2D-sheet and 1D atomic wire of Silicon, using the Full Potential Linearized Augmented Plane Wave method (FP-LAPW) within the framework of DFT. The electron exchange correlation was treated with the modified Becke-Johnson exchange potential (PB-mBJ) for bulk Silicon and for Si sheet and wire, the most common Generalized Gradient Approximation (GGA) is taken into consideration. The transport coefficients were calculated by a post DFT treatment which involved the semi-classical Boltzmann Theory as implemented in the code BoltzTraP. For Si, we observed that as we move towards lower dimensionality, the thermoelectric efficiency ZT increases significantly (bulk ~ 0.01 , Si sheet ~ 1.1 and Si wire ~ 1.65 at 300 K). The increase in ZT is mostly due to the change in phase in going from higher to lower dimension, which increases the electrical conductivity and reduces the thermal conductivity. Results obtained are compared with available theoretical and experimental results.

Keywords: Thermoelectric properties, 1D atomic silicon, 2D sheet silicon, FP-LAPW, DFT, Becke-Johnson exchange potential, BoltzTraP.

1. Introduction

Thermoelectric materials are gaining tremendous attention because it plays an important role in energy conversion between heat and electricity, an alternative source for green energy production [1]. With the exhausting global energy consumption rate, a new renewable and environmentally friendly energy resource is a challenge [2]. The utilization of huge quantity of fuel in the industries and factories has degraded the amount of energy supply. On the other hand, the by-product from these factories is the large amount of heat [3]. Thermoelectric materials can directly convert heat into electricity and are thus being considered as the solution of the world's energy crisis [3]. The efficiency of a thermoelectric material is defined by its dimensionless Fig. of merit ZT , given by,

*) For Correspondence. E-mail: dibyaprakashrai@gmail.com

$$ZT = \frac{\sigma S^2}{\kappa_e + \kappa_p} T \quad (1)$$

where, σ is the electrical conductivity, S is the Seebeck coefficient, defined as the measure of the magnitude of induced thermoelectric voltage in response to a temperature difference [4], κ_e is the electronic contribution to thermal conductivity and κ_p is the phonon contribution to thermal conductivity.

In this work, silicon is explored as a thermoelectric material due to its abundance, established manufacturing infrastructure, high temperature stability and negligible toxicity. Our main objective is to study the thermoelectric properties of silicon atomic wires, sheet and bulk, and their applications in producing the usable amount of standard electricity by utilizing the waste heat. However, the technology has not progressed far enough to make this a reality. The fundamental problem is that for a material to be an efficient thermoelectric it needs to be a good conductor of electricity, but not heat. Otherwise, the device will reach thermal equilibrium and the generation of electricity will cease [5]. Unfortunately, in most materials, thermal and electrical conductivity tends to go hand in hand. Thus to decouple electrical and thermal conductivity is a great technological challenge. As with most material properties, controlling the micro-structure is the key to optimizing thermoelectric performance [3]. There are many theoretical models [6] for increasing the efficiency of the materials, however, the most effective models being used are the super-lattice or quantum well structures [7] and nano-structured engineering [8].

Low dimensionality can be largely beneficial for increasing the thermoelectric properties as it increases the power factor of a material [9]. Recently, large improvements in ZT have been reported in silicon nano wires ($ZT \sim 1$) compared to the bulk ($ZT \sim 0.01$) [3, 10]. We have investigated the electronic band structure and thermoelectric parameters like Seebeck coefficient (S), electrical conductivity (σ/τ) and electronic thermal conductivity (κ/τ) of silicon bulk, sheet and 1-D wire. The electronic band structure is directly related to S of the material and S to the thermoelectric parameters. For all three cases, the value of S is very low; this is because of the absence of dense and narrow band gap at or around Fermi level [11]. However, high ZT values of Si-wire and Si-sheet are caused by the reduction of κ due to decrease in dimensionality. We have neglected in our ZT calculation due to lack of data, thus, modifying the efficiency equation to

$$ZT = \frac{\sigma S^2}{\kappa} T, \text{ where } \kappa = \kappa_e.$$

2. Model and Calculation Method.

We have performed the first principle calculations based on the Density Functional Theory (DFT) using the WIEN2k code [12]. The electronic structure calculation was performed using the modified Becke-Johnson exchange potential (PB-mBJ) [13] and Generalized Gradient Approximation (GGA) [14] based on the Full Potential Linearized Augmented Plane Wave (FPLAPW) method [15, 16]. The natural output of energy band from the first principles calculation is taken as the key input for the calculation of transport properties, as implemented in the program code BoltzTraP [17].

The monatomic Si-nano wire was designed using the super cell method in which the position of Si atom was taken based on orientation (0.5, 0.5, 0.5) and a vacuum of 20 Å was applied along the x- and y-axis in order to discontinue the atomic wave function and to

break the crystal symmetry along the x-and y-direction. As a result, the repetition of the Si-atom takes place only along one direction i.e. along the z-axis. The obtained structure is a 1D Si atomic chain (periodic linear chain of identical atoms) as shown in Fig. 1(c). The preparation of Si-wire is similar to that of Fe-wire [18]. The lattice constants (a and b) of the Si-wire have been changed to 20 Å and the lattice constant of c is 1.92 Å which is equivalent to the bond length. Similarly, for Si sheet, a vacuum of 10 Å was applied along the z-axis to break the crystal symmetry along the z-direction, as shown in Fig. 1(b). The lattice constants (a and b) of the Si-wire are taken as 3.82 Å and the lattice constant of c is taken as 10 Å. The bulk-Si crystallizes in FCC structure with lattice constants, $a = b = c = 5.431$ Å [19], is shown in Fig. 1 (a).

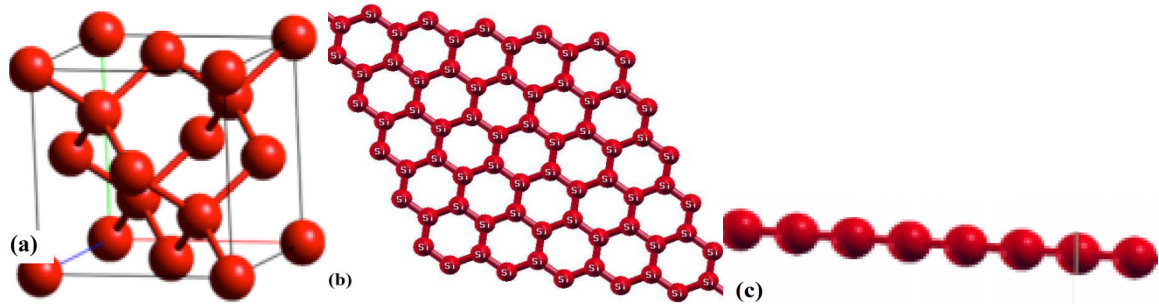


Fig. 1: (a) FCC crystal structure of bulk silicon (b) 2-D Si sheet and (c) 1-D silicon atomic chain

3. Results

3.1 X-ray Diffraction

It is necessary to obtain a good description of electronic structure in order to determine the thermoelectric properties. The contribution of different electronic states in the valence and the conduction band determines the electronic property of the material. This is shown with the help of band structure along with the density of states in following Figs. 2(a-c).

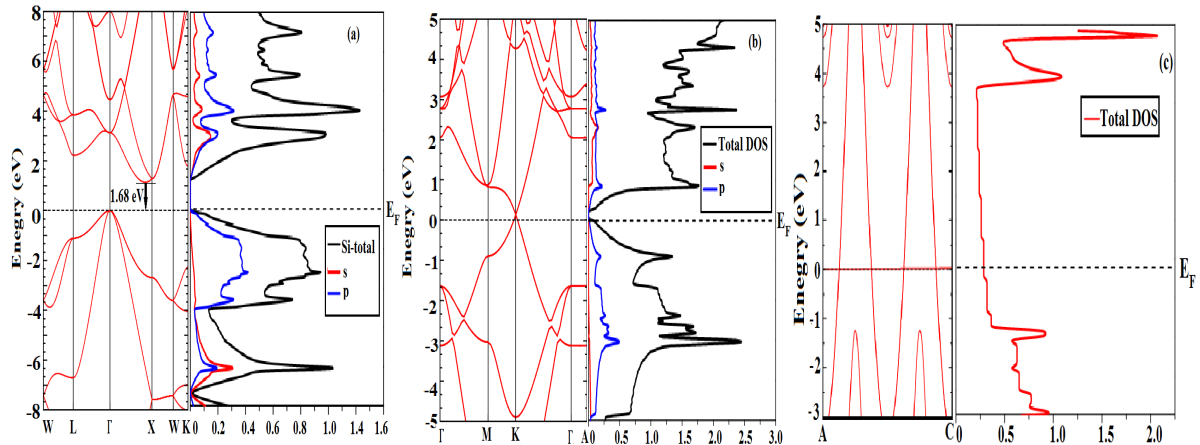


Fig. 2: (a) band structure of bulk silicon crystal (b) band structure of 2-D silicon sheet and (c) band structure of 1-D silicon atomic wire.

The band structure of bulk silicon is shown in Fig. 2 (a). An indirect band gap of 1.68 eV along Γ -X symmetry was observed, which is in close agreement with those obtained by many authors [20, 21, 22]. The presence of small band gap in bulk Si indicates its

semiconducting nature. In the case of Si sheet, the Fermi level, E_F cuts the DOS slightly in the valence region, as shown in Fig. 2(b). The band in the E_F along K-symmetry is due to the overlapping of p-states of Si. Similar trends in band structure and DOS has been reported by Behera *et al.* [23]. However they have obtained a different value of the band gap for bulk Si, this may be due to the difference in energy exchange potential.

The band structure and DOS calculated from GGA for Si atomic wire is shown in Fig. 2(c). The total DOS extends from -3 eV to 5 eV. The states above 5 eV are completely unoccupied due to the vacuum applied in order to discontinue the atomic wave function. In our previous study [24], we had observed a Dirac cone like feature at about 3 eV above the Fermi energy along the Δ -symmetry. The band structure is different in this study since we have considered the dispersion relation of phonon, applying a different wave vector, K_z which was expected to increase the ZT of the wire. The band structure of Si wire indicates metallic nature, which is in agreement with the previous study [25]. In the case of Si atomic chain, the cone-like features are shifted entirely to the conduction region, showing almost narrow band gap. The shifting of the narrow band gap in Si-wire indicates the existence of an intermediate state between metal and semiconductor. The transformation of the band gap into an overlapping energy band, with the decrease in the dimensionality of a material, increases the electrical conductivity. Furthermore, it reduces the lattice thermal conductivity, which finally leads to an increase in ZT.

3.2 Thermoelectric properties

The existence of crystalline phase was verified by SEM analysis. Fig. 2(a)-(d) show the SEM micrographs of some $\text{TeO}_2 - \text{Na}_2\text{O} - \text{MgO}$ glass systems in varying Eu_2O_3 dopant concentration. Some of them are spherical in shape, some have star-like structure and some of them are irregular in shape. All the micrographs confirm that the crystalline region is composed of TeO_2 phase is dominant.

$$S = \frac{\pi^2 k_B^2 T}{3e} \left(\frac{d\{\ln[\sigma(E)]\}}{dE} \right)_{E=E_F}$$

The value of calculated Seebeck coefficient (S) is plotted against temperature which is shown in Fig. 3(a). The value of S at 300K for Si-bulk, sheet and wire are $1.96\text{E-}05$, $-7.63\text{E-}04$ and $-9.37\text{E-}05$ V/K respectively. The low value of S in our calculation is due to the absence of the dense bands near E_F in the band structure [26]. The nature of the carriers can be predicted by the sign of the Seebeck coefficient. The magnitudes of S along the negative and positive side are equal, which indicates the equal number of n/p-type carriers for Si-2D sheet and Si-bulk. However, the magnitude of S in the negative side is higher, indicating the n-type carriers in the Si-1D wire. The mixed carrier concentration is observed for bulk, which is the reason for its low ZT value. For temperatures up to 500 K, the carrier concentration is negative, and for higher temperatures, the carrier concentration is positive, as shown in Fig. 3(a). To ensure that the Seebeck coefficient is large, there should only be one type of carrier. Mixed n and p-type conduction will lead to both charge carriers moving to the cold end, canceling out the induced Seebeck voltage [1]. The plot of Seebeck coefficient against temperature increases up to the room temperature (300 K) and then the slope decreases, which is a typical behavior of low carrier density metal [27]. This is in agreement with our previous study [24].

The variation of an electrical conductivity against temperature is shown in Fig. 3(b). It can be seen that the electrical conductivity of atomic wire is almost constant with temperature, in fact, it decreases slightly with the increase in temperatures (above room temperature), whereas electrical conductivity is expected to increase with temperature. This result deviates from our previous result. This may be due to the inclusion of phonon dispersion. The variation of thermal conductivity with temperature is shown in Fig. 3(c). Is very low for Si sheet and increases with the increase in temperature. We observed that for higher temperatures, value for Si wire and sheet coincides. For Si-wire the value decreases with the increase in temperature and this led to its high ZT value. This may be because of deficiency in the number of electrons in order to transport heat in 1D structure. Fig. 3(d) gives the variation of the figure of merit with temperature. The ZT value calculated at 300K for bulk, sheet and wire are 0.013, 1.11 and 1.64 respectively. For both Si-sheet and wire, the ZT value decreases with the increase in temperature. This is because, for Si-sheet, increases abruptly with temperature, thus decreasing ZT and for Si-wire, the reason being the decrease in conductivity with temperature. An improved ZT is obtained for Si-wire in comparison to our previous study [24].

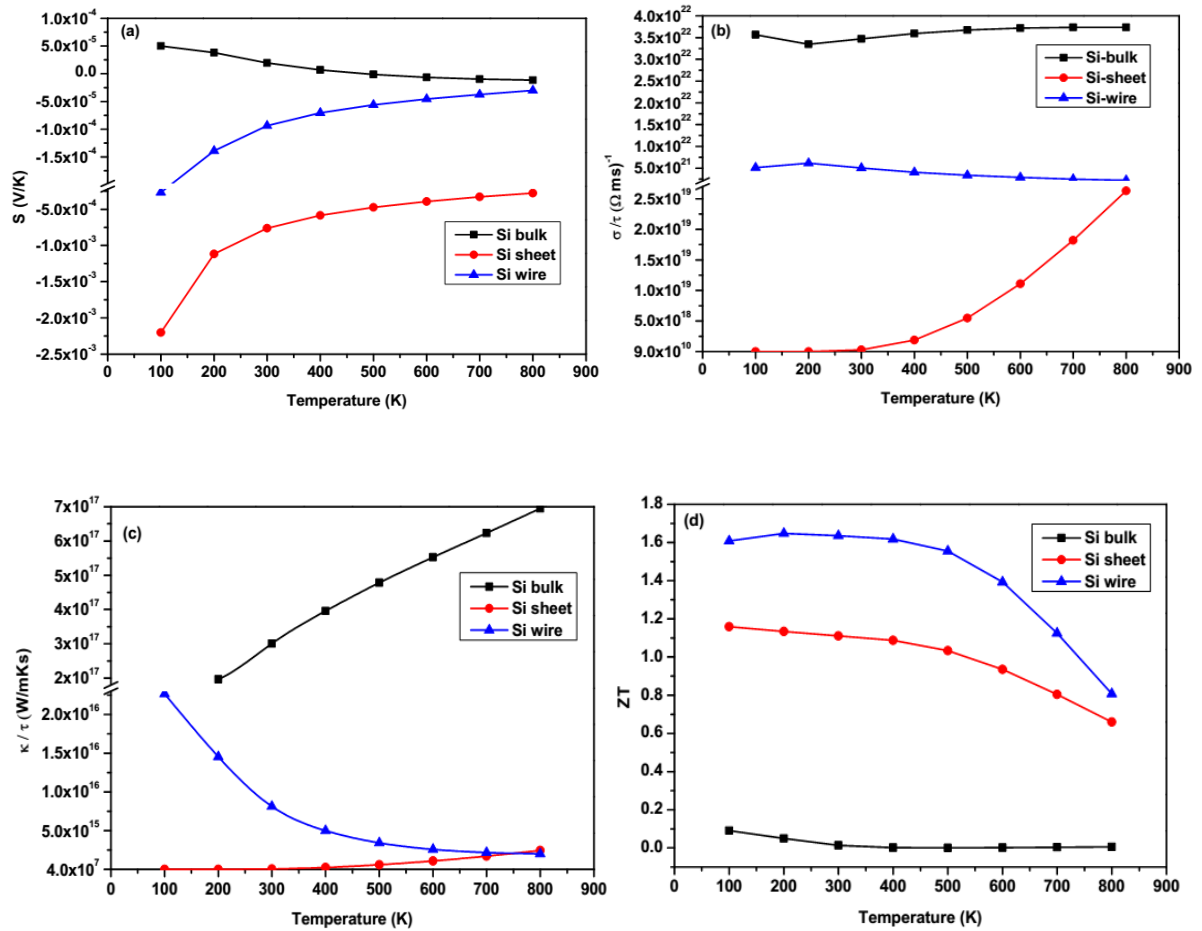


Fig. 3: (a) Temperature dependence of Seebeck coefficient (S), (b) electrical conductivity over relaxation time (σ/τ), (c) electron thermal conductivity (k) and (d) Fig. of merit (ZT).

4. Conclusion

The formation of cone-like features in the case of Si-nano material, which is absent in bulk materials indicates the presence of high effective mass and favors high ZT value. This also implies to a change in phase to an intermediate state between metal and semiconductor, which is the reason for the increase in electronic conductivity. The intrinsic conductivity and intrinsic carrier concentration are largely dependent on the ratio of band gap to the temperature. When this ratio is large, the concentration of intrinsic carriers will decrease and the conductivity will also decrease. In the case of silicon sheet and wire, no band gap is observed, that the ratio is almost zero, thereby, increases the concentration of intrinsic carrier and also its conductivity. Thus both Si sheet and atomic wire is a good candidate for the thermoelectric purpose. The drawback of our code lies in the exclusion of phonon contribution to thermal conductivity. Our thermoelectric efficiency result is only based on the contributions by electrons. The inclusion of phonon effect may reduce the thermoelectric efficiency. Furthermore, the inclusion of dopants, in addition to the reduction in structural dimensionality could reduce the hole concentration in the material and increase the Seebeck coefficient, hence increase the ZT value.

Acknowledgments

This part of the work was done as an M.Sc project by Mr. H. Joshi under the supervision of Prof. R. K. Thapa. HJ and RKT acknowledge research project grant from SERB (Govt. of India) EMR /2015/001407.

References

- [1] G. Jeffrey Snyder and Eric S. Toberer, *Nature Materials*, **7**, 105-114 (2008)
- [2] Jin-cheng Zheng, *Front. Phys. China*, **3** (3), 269-279 (2008)
- [3] A. I. Hochbaum, R. Chen, R. D. Delgado, W.Liang, E.C. Garnett, M.Najarian, A.Majumdar and P.Yang, *Nature* **451**, 163-168 (2008)
- [4] T. J. Seebeck, *Ostwald's Klassiker der Exakten Wissenschaften*, **70**, 1822-23 (1895)
- [5] Li-Dong Zhao, Shih-Han Lo, Yongsheng Zhang, Hui Sun, Gangjian Tan, Ctirad Uher, C. Wolverton, Vinayak P. Dravid and Mercouri G. Kanatzidis, *Nature*, **508**, 373-379 (2014)
- [6] G. Mahan, B. Sales and J. Sharp *Phys. Today*. **50** 42(1997)
- [7] S. J. Youn and A. J. Freeman, *Phys. Rev. B***63** 085112, 1- 4 (2001)
- [8] A. Majumdar, *Science*, **303**, 777 (2004)
- [9] L.D. Hicks, and M. S. Dresselhaus, *Phys. Rev. B*, **47**, 16631 (1993)
- [10] A.I. Boukai, Y. Bunimovich, J. T.-Kheli, J.-K. Yu, W. A. G. III, and J. R. Heath, *Nature*, **451**, 168-171 (2008)
- [11] Joseph P. Heremans, Vladimir Jovovic, Eric S. Toberer, Ali Saramat, Ken Kurosaki, Anek Charoenphakdee, Shinsuke Yamanaka, G. Jeffrey Snyder, *Science*, **321**, 554-557 (2008)
- [12] P. Blaha, G.K.H. Madsen, D. Kvasnicka, J. Luitz, WIEN2K, an augmented plane wave plus local orbitals program for calculating crystal properties (Vienna, Austria) 2008
- [13] J. A. Camargo-Martínez and R. Baquero, *Superficies y Vacío* **26** (2), 54-57, 2013
- [14] J Perdew, K P Burke and M Ernzerhof *Phys. Rev. Let.* **77** 3865 (1996)
- [15] M. Hyberstsen, M. S. Schluter and N. E. Christensen *Phys. Rev. B***39**9028 (1989)
- [16] E. Wimmer, H. Krasauer, M. Weinert and A. J. Freeman *Phys. Rev. B***24**864 (1981)

- [17] G. K. H. Madsen and D. J. Singh *Comput. Phys. Commun.* **175**67 (2006)
- [18] D. P. Rai, Sandeep, A. Shankar, P. K. Patra and R. K. Thapa, *Nanoscience and Nanoengineering*, **4**, 52 - 57 (2016)
- [19] T. Hom, W. Kiszenik and B. Post, *J. Appl. Cryst.*, **8**, 457-458 (1975)
- [20] J. C. Phillips, *Phys. Rev.* **125**, 1931-1936, (1962)
- [21] Manuel Cardona and Fred H. Pippard, *Phys. Rev.*, **142**, 530-543, (1966)
- [22] James R. Chelikowsky and Marvin L. Cohen, *Phys. Rev. B***10**, 5095-5107, (1974)
- [23] H. Behera and G. Mukhopadhyay “A comparative computational study of the electronic properties of planar and buckled silicone” presented in Workshop on New and Nano Materials (WNNM)-2012, Institute of Materials Science, Planetarium Building, Bhubaneswar-751013, Odisha
- [24] H. Joshi, D. P. Rai, P. K. Patra, K. C. Bhamu, R. K. Thapa, *Nanoscience and Nanoengineering*, **4**(4): 59-63 (2016)
- [25] T. Yamada, *J. Vac. Sci. Technol.* **B15**, 1019 (1997)
- [26] Ashcroft and Mermin, *Solid State Physics*, Holt, Rinehart and Winston, 1976
- [27] Kengo Kishimoto, Masayoshi Tsukamoto, and Tsuyoshi Koyanagi, *Journal of Applied Physics* **92**, 5331 (2002)

